THE ABUNDANCE DISCREPANCY FACTOR AND t^2 IN NEBULAE: ARE NON-THERMAL ELECTRONS THE CULPRITS?

G. J. Ferland[1], W. J. Henney[2], C. R. O'Dell[3], M. Peimbert[4]

RESUMEN

La fotoionización produce electrones supratérmicos, electrones mucho mas energéticos que los que se encuentran en un gas termalizado con una temperatura electrónica característica de nebulosas gaseosas. La presencia de estos electrones de alta energía podría resolver: a) la discrepancia entre las abundancias obtenidas a partir de líneas prohibidas y las obtenidas a partir de líneas de recombinación (problema t^2/ADF), y b) que los diferentes indicadores de temperatura den valores diferentes. Esto sería posible si los electrones supratérmicos sobreviven el tiempo suficiente para afectar las líneas de emisión. Usamos métodos bien establecidos para mostrar que las distancias en que las tasas de calentamiento cambian son mucho mayores que las distancias que pueden viajar los electrones supratérmicos, y que las escalas de tiempo para termalizar a estos electrones son mucho menores que las escalas de calentamiento o enfriamiento. Estas estimaciones implican que los electrones supratérmicos se maxwellianizan mucho antes de que puedan afectar a las líneas prohibidas colisionalmente excitadas y a las líneas de recombinación que se usan para obtener las abundancias relativas. La distribución electrónica de velocidades en las nebulosas debe ser muy cercana a la Maxwelliana.

ABSTRACT

Photoionization produces supra-thermal electrons, electrons with much more energy than is found in a thermalized gas at electron temperatures characteristic of nebulae. The presence of these high energy electrons may solve the long-standing t^2/ADF puzzle, the observations that abundances obtained from recombination and collisionally excited lines do not agree, and that different temperature indicators give different results, if they survive long enough to affect diagnostic emission lines. The presence of these non-Maxwellian distribution electrons are usually designated by the term kappa. Here we use well established methods to show that the distance over which heating rates change are much longer than the distance supra thermal electrons can travel, and that the timescale to thermalize these electrons are much shorter than the heating or cooling timescales. These estimates imply that supra thermal electrons will have disappeared into the Maxwellian velocity distribution long before they affect the collisionally excited forbidden and recombination lines that are used for deriving abundances relative to hydrogen. The electron velocity distribution in nebulae should be closely thermal.

Key Words: atomic processes — galaxies: active — methods: numerical — molecular processes — radiation mechanisms

[1]Department of Physics and Astronomy, University of Kentucky, Lexington, KY 40506, USA

[2]Centro de Radioastronomía y Astrofísica, Universidad Nacional Autónoma de México, Apartado Postal 3-72, 58090 Morelia, Michoacán, México

[3]Department of Physics and Astronomy, Vanderbilt University, Box 1807-B, Nashville, TN 37235

[4]Instituto de Astronomia, Universidad Nacional Autónoma de México, Apdo, Postal 70-264, 04510 México D. F., México

1. INTRODUCTION

The electron kinetic temperature is one of the most fundamental characteristics in a photoionized nebula such as an H II region or a planetary nebula. These temperatures are derived from ratios of emission lines in the optical spectrum and this methodology has been a major tool in the analysis of the nebular spectra for 60 years (Osterbrock 2002). These temperatures are usually about 10,000 Kelvin and are called the electron kinetic temperatures (T_e) since they reflect the energy distribution of the free electrons in the gas. T_e is different from other temperatures encountered in the treatment of a nebula, e.g. the ionizing star temperature, the ionization temperature, and the excitation temperature derived from the ratio of populations in atomic levels. If one knows T_e, one can then use other emission lines to determine the relative abundance of different atoms, a process reviewed in Osterbrock & Ferland (2006), hereafter AGN3.

Collisionally-excited forbidden lines of the heavy elements are often the strongest lines in a nebula's spectrum. Their emissivity increases sharply with higher T_e. This is in contrast with lines produced during the recombination of electrons with ions, where the emissivity increases with lower T_e. While hydrogen and helium recombination lines are strong, recombination lines of the heavy elements are usually weak in the observed spectrum because their strength approximately scales with their relative abundance. Because of the different temperature dependencies, abundances determined from ratios of recombination lines will be far less temperature sensitive than those determined from the ratio of collisionally excited and recombination lines. The state of the art is that faint forbidden and recombination lines from heavy elements can now be measured and abundances from the two methods compared (Peimbert 2003; Esteban et al. 2004).

There is a long-standing riddle when applying T_e for the determination of abundances relative to hydrogen. One generally derives higher relative abundances from recombination lines than from the forbidden lines. This is called the "abundance discrepancy factor" (ADF) problem, and a possible origin lies in temperature fluctuations, parameterized as "t^2" (Peimbert 1967; Peimbert et al. 1993). The presence of temperature fluctuations causes the abundances determined from the forbidden lines to underestimate the abundances, accounting for the ADF.

The ADF or t^2 problem is largest in planetary nebulae, with an ADF sometimes more than an order of magnitude (Liu et al. 2000). It is smaller in H II regions, such as the Orion nebula, but the ADF is still nearly a factor of two (Peimbert & Peimbert 2013). The t^2 values predicted by photoionization models with constant density are in the 0.002 - 0.02 range with typical values around 0.004, while in many cases the t^2 observed values are higher, in the 0.02 to 0.05 range. Large temperature fluctuations could be caused by many processes including a) density fluctuations, b) shocks, c) shadowed regions, d) chemical composition inhomogenieties, or e) variations in the fluxes from the ionizing stars. These fluctuations are caused by real changes in temperature caused by different regions contributing along a line of sight and within the spatial resolution of the observations, with each region having a well defined electron kinetic temperature corresponding to a Maxwellian velocity distribution.

One suggestion to account for t^2, discussed in three recent papers, is that the free electrons in the ionized gas do not have a thermal velocity distribution (Nicholls et al. 2012, 2013; Dopita et al. 2013). These authors propose that a significant population of supra-thermal electrons exist in the ionized gas. They use the "kappa" formulation (Vasyliunas 1968) to describe the velocity distribution of these non-thermal electrons. The assumption of kappa is attractive because such a distribution would have more high velocity electrons than a Maxwellian distribution. These high-velocity electrons would be more effective in collisional excitation of the metastable levels that produce the forbidden lines of heavy elements, but particularly those of auroral lines, whose relative strength is critical in determining T_e. This would mean that the temperature determined assuming a Maxwellian distribution will be over-estimated; therefore the emissivity of the nebular forbidden lines will be over-estimated and the relative abundance of the heavy elements will be systematically underestimated. This would also explain the ADF.

However, the assumption that non-thermal electrons could survive in an ionized gas long enough to affect the spectrum has not been critically examined. We know of no detailed numerical calculation that follows the evolution of a non-thermal electron in an ionized gas. This has not been done since the arguments outlined below suggest that this is not necessary. Below we outline the processes and timescales that characterize a photoionized gas such as an H II region or planetary nebula. These are based on the rigorous treatment of the rates of collisions and recombinations that apply to an ionized

gas. These rates determine the time scale and distance over which a non-thermal electron distribution would disappear. They show that the forces establishing a thermal distribution are powerful and far faster than those that disturb the distribution.

In Section 2 we describe the basic characteristics of a thermal gas and a kappa gas, and in Section 3 we identify where kappa may play a role. Section 4 describes heating and ionization processes in photoionization while Section 4.2 gives typical numbers for the photo ionization physics for the Orion Nebula, a characteristic H II region. In Section 5 we discuss what would happen if there are kappa electrons, and we summarize our conclusions in Section 6.

2. ELECTRON VELOCITY DISTRIBUTIONS IN A THERMAL GAS AND A KAPPA GAS

In a collisionless gas, a gas where particles do not collide with one another, electrons will maintain whatever energy and velocity they originally have. Collisions between particles causes them to share kinetic energy, and if a sufficient number of collisions occur, they will reach energy equipartition. Particles in a thermal gas have undergone a sufficient number of collisions to have reached this equilibrium and the distribution of velocities is given by the Maxwellian distribution function. This distribution has a most frequent velocity with exponential tails at high and low velocities. Such a distribution is shown as the dashed line in Figure 1. This physics is covered in, for instance, Spitzer (1962).

This is quite different from a kappa gas, where the electron distribution function has an excess at high energies and velocities, as shown by the solid line in Figure 1. This must happen to some extent since photo electrons enter the gas at a high velocity and then decay to lower velocity. After enough collisions, the signature of the kappa gas disappears as the history of the injected electrons is erased.

To explain typically observed ADF values, kappas in the 20 to 50 range are required. Moreover the effect of kappa can be reproduced with temperature variations of the magnitude

$$t^2 = 0.96/\kappa \qquad (1)$$

(Peimbert & Peimbert 2013). Values of kappa larger than 1000 produce negligible ADF values.

As described in the following sections, high-energy photoelectrons are continuously entering the plasma, so to some extent a high-energy kappa tail will be present. The key question is how important
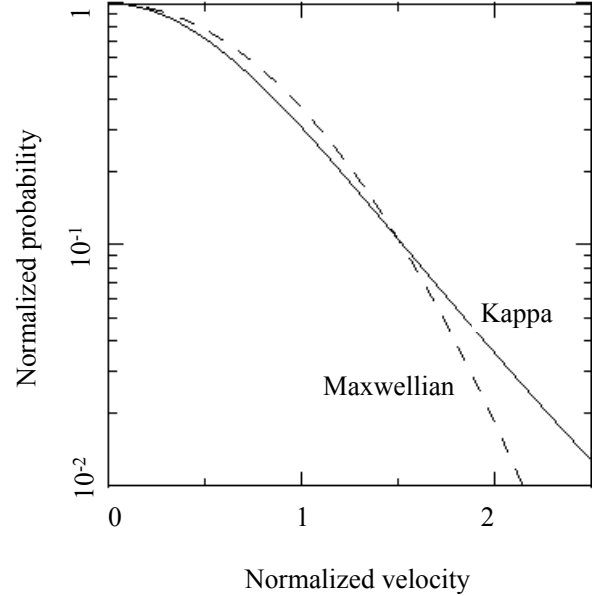

Fig. 1. Comparing a Maxwellian with a kappa electron velocity distribution. The kappa distribution has more high-energy electrons than a thermal gas. Smaller values of kappa correspond to greater deviations from a Maxwellian while a thermal distribution has a kappa of infinity. Equation 1 shows the relation between t^2 and kappa.

these high-energy electrons are relative to the thermal electrons. This comes down to a question of timescales - how does the thermalization timescale, the time required for a high-energy electron to become thermal, compare with the rate non-thermal electrons are introduced into the gas, or for them to affect the forbidden lines? We address this by examining timescales for equilibrium in a photoionized gas in the following sections.

3. WHERE NON-THERMAL VELOCITY DISTRIBUTIONS APPLY, AND TESTS TO DETERMINE THIS

This section outlines three regions where suprathermal electrons are known to be important, and discusses the tests used to diagnose this condition.

Non-thermal electron distributions are important in active regions of the sun, as reviewed by Bradshaw & Raymond (2013). Flares are regions where suprathermal electrons are created by the explosive release of energy following magnetic reconnection. These very high energy electrons interact with atoms before they have time to relax. A *timescale test* is applied to determine whether suprathermal or kappa electrons will be important. Such tests show that flare electrons will be non-thermal.

Non-thermal particle distributions are also important in certain types of shocks, also reviewed by Bradshaw & Raymond (2013). This is most important in low-density neutral regions where the mean free path becomes large compared with the dimensions in the system. The most important effect is when cold neutral atoms pass through a shock and become ionized in warm ionized regions downstream. These cold protons can emit before undergoing enough collisions to become thermal. Details of the resulting non-Maxwellian velocity distribution, for protons, are given by Raymond et al. (2008). In this case a *length test* that compares the mean free path and the dimension for changes in the system is applied and shows that non-thermal distributions are important.

The kappa formalism is only one way of dealing with non-thermal electrons. Most spectral simulation codes, including Cloudy (Ferland et al. 2013), solve for a population of suprathermal electrons and include them as a general excitation process. Suprathermal electrons are known to be important when high-energy photons enter neutral regions such as the H^0 or H_2 phases of star-forming regions (Chapter 11 of AGN3). In this case high-energy photoelectrons, or cosmic rays, can excite and ionize the gas before undergoing enough elastic collisions to be thermalized. This is due to the low electron fraction, making it more likely that a suprathermal electron will collide with an atom or molecule before undergoing thermalizing collisions with electrons.

These suprathermal electrons, sometimes called "secondary" or "knock-on" electrons, have been treated in Spitzer & Tomasko (1968); Bergeron & Collin-Souffrin (1973); Shull (1979); Xu & McCray (1991); Shull & van Steenberg (1985); Dalgarno et al. (1999). The kappa distribution is not used although the idea is similar. Cloudy has included this physics since its birth in 1978. The test here is the *ionization fraction*, proportional to $n(H^+)/n(H)$, with suprathermal electrons being important in neutral regions such as X-ray illuminated PDRs, often called XDRs (Maloney et al. 1996).

To summarize this discussion, thermal distributions are established by elastic electron - electron collisions (Chapter 2, Spitzer 1978). The question whether non-thermal electrons will be important in an H II region is really a question of time scales, length scales, and ionization fractions. Relevant scales in a typical H II region, the Orion nebula, are discussed next.

4. THE PRIMARY MECHANISM IN PHOTOIONIZED NEBULAE

We accept that H II regions and planetary nebulae are photoionized by starlight. The photoionization process will be the main source of high-energy electrons in such nebulae. As described above, the central question is how quickly, and over what scales, these suprathermal electrons survive before they become thermal. First we consider some basic properties of a photoionized cloud.

The primary mechanism[5] is the process whereby photoionization converts high-energy portions of a stellar SED into an emission-line spectrum. It is shown schematically in Figure 2. In this Figure, taken from AGN3, the SED of an active galactic nucleus is shown in the left part of the Figure. The rightward pointing arrow shows the energy range of photons which are capable of photoionizing hydrogen. Ionizing photons are absorbed by atoms in a gas cloud, producing energetic photoelectrons, whose energy is the difference between the ionizing photon and the ionization energy of the atom (AGN3 Chapter 2). These energetic electrons collide with thermal electrons and protons to eventually become thermal. The free electrons produce collisionally excited forbidden emission lines through inelastic collisions with heavy elements, and briefly become subthermal electrons. They eventually recombine with an ion, producing recombination emission lines. The emission-line spectrum shown in the right of Figure 2 results.

4.1. *Details of the Primary Mechanism*

It is commonly assumed that supra or subthermal electrons share their energy with surrounding electrons so quickly that they become thermal electrons long before exciting one of the forbidden lines of the heavy elements. Bohm & Aller (1947) were the first to consider this in detail, while Spitzer & Härm (1953) and Bhatnagar et al. (1954) go into more details. This is now textbook material; Spitzer (1962) discusses electron transport at length, while Spitzer (1978) and Kulsrud (2005) summarize it more briefly.

The energy of the photoelectron produced by the photoionization of hydrogen is central to these timescale questions. Figure 3 compares the SEDs of three different ionizing continua. The curve with fine structure is the spectrum of an O star similar to the ionizing stars in the Orion Nebula. The smoothest

---

[5]The term "primary mechanism", photoionization by the radiation field of the central object, dates back to the 1930's and the original investigations into nebulae.
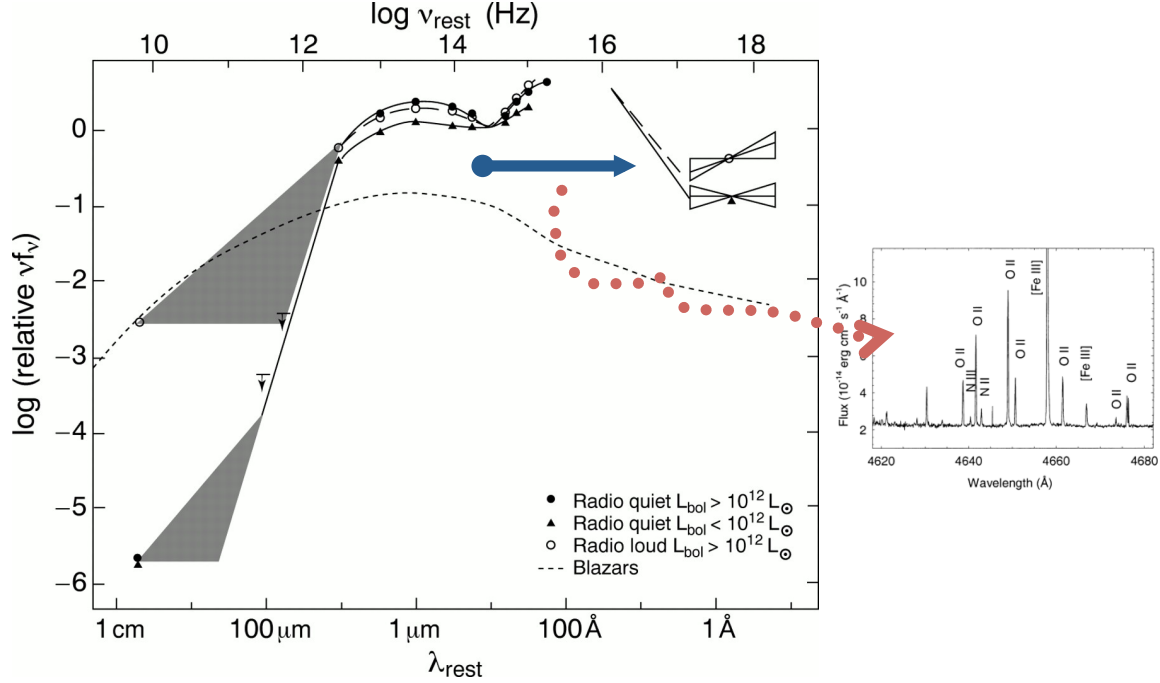
Fig. 2. The "primary mechanism", converting an SED into emission lines.

line extending to the shortest wavelengths and highest energies is the SED produced by the central black hole of an AGN. The central star of the planetary nebula is the intermediate SED. The vertical line in the figure indicates the ionization potential of hydrogen. These shapes determine the energy of the photoelectron since an ionizing photon produces a photoelectron with an energy equal to the difference between its energy and this ionization potential. The AGN continuum will produce the most energetic photo-electrons while the O star continuum the least.

We can quantify this by considering an average of the photoelectron energy, $h(\nu - \nu_0)$, where $h\nu$ is the ionizing photon energy and $h\nu_0$ is the ionization potential, weighted by the photoionization cross section α_ν. We can express this photoelectron energy as an equivalent temperature:

$$\langle h(\nu - \nu_0)\, \alpha_\nu \rangle = \frac{\int_{\nu_0}^{\infty} \frac{4\pi J_\nu}{h\nu} h(\nu - \nu_o)\alpha_\nu \, d\nu}{k \int_{\nu_0}^{\infty} \frac{4\pi J_\nu}{h\nu} \alpha_\nu \, d\nu} \qquad (2)$$

where k is Boltzmann's constant. Table 1 gives this mean. The first column gives the SED label. The O star is the softest of the three continua, producing photoelectrons with a kinetic energy equivalent to 53 kK, the planetary nebula is intermediate, and the active galactic nucleus is the hardest SED with 321 kK.

TABLE 1

PHOTOELECTRON ENERGIES FOR THE THREE SEDS.

SED	$\langle h(\nu - \nu_0)\rangle k^{-1}$	
H II	52.7 kK	4.54 eV
PN	266 kK	22.9 eV
AGN	321 kK	27.7 eV
Thermal	10 kK	0.862 eV

For comparison the typical gas kinetic temperature in the surrounding nebulae will be about 10k K. Going back to Figure 1, a typical photoelectron would be off-scale to the right, typically $5-30\sigma$ away from the mean of the Gaussian. The central question is, then, whether this high-energy photoelectron can become thermal before producing an emission line that we would use as a diagnostic indicator.

4.2. History of an Electron in the Orion Nebula

We focus on H II regions because of their role in measuring galactic nucleosynthesis. We consider physical processes in the Orion H II region, a bright and well studied H II region with a density of $n(\mathrm{H}) \sim 10^4 \, \mathrm{cm}^{-3}$. We focus on the model of the bright inner regions developed by Baldwin et al. (1991) and further discussed by Ferland (2001) and Ferland (2003). We consider the life history of hydrogen and its electron at the midpoint in the H^+ region shown in Fig-
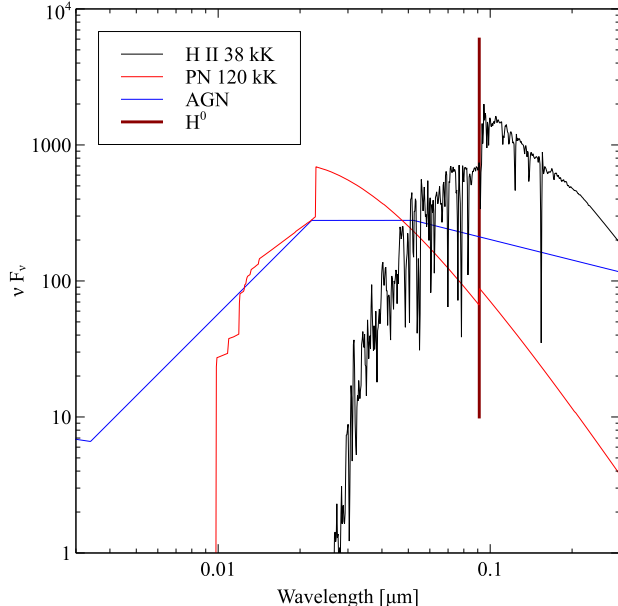
Fig. 3. The SEDs of an O star, a PN central star, and a typical AGN, as shown. The vertical line indicates the ionization potential of hydrogen.

ure 2 of Ferland (2003). This will establish numbers for the time and distance scale tests.

A neutral hydrogen atom located at this point will survive for roughly a day before an ionizing photon from the Trapezium Cluster causes a photoionization. This generates a photoelectron whose typical energy is given by $h\nu - IP \approx 53$ kK. The photoelectron is suprathermal because it has more energy than the surrounding thermal electrons, $kT \approx 10$ kK.

The supra-thermal electron remains very energetic for about a second before it shares its energy with other free electrons in the gas and becomes thermal. The energy exchange occurs through electron - electron collisions, which are among the fastest collisions in an ionized gas. They are also perfectly elastic because little radiation is produced in a homonuclear collision, a result of the lack of a dipole moment. This process is referred to as the thermalization of the supra-thermal electron.

The electron will remain a thermal free electron for about ten years. During this time it may collide with ions, probably O^{2+} or O^+ since oxygen is the third most abundant element and these are the dominant ionization stages. The thermal electron will excite an internal level of the oxygen ion and such levels can decay and emit the strong optical lines that are prominent in nebulae. Such collisions happen about once a month. After the collision, the free electron will have lost a great deal of its kinetic en-

ergy, becoming sub-thermal, but regains the energy following collisions with other free electrons. The free electron is rethermalized within about a second.

After about ten years the free electron will have a near encounter with a proton, be accelerated and radiate much of its kinetic energy, and recombine forming H^0. Electrons tend to be captured into highly excited states which have lifetimes of about 1×10^{-5} s to 1×10^{-8} s so the electron quickly falls down to the ground state. The electron remains in the ground state for about a day before another ionizing photon is absorbed and the process starts again. This is the primary mechanism in nebulae and summarizes the competing processes that determine the electron velocity distribution. A summary of the timescales for the most important components of a nebular plasma are given in Table 2, where one sees that collisions with electrons are the most frequent.

4.3. A question of time and length scales

There are two tests to check whether an electron will undergo sufficient collisions to become thermal. The *distance test* checks whether the local photoelectric heating rate changes over distances that are smaller than the electron thermalization mean free path. The *time scale test* checks whether the photoelectric heating rate changes more quickly than the electron thermalization timescale.

First compare the heating scale length with the electron mean free path. Heating is by starlight photoionization. The mean free path of an H^0-ionizing photon is

$$\lambda_{912} = [n(H^0)\sigma(H^0)]^{-1}. \qquad (3)$$

We must compare this with the electron thermalization scale

$$\lambda_{e-e} = [n_e \sigma_{e-e}]^{-1}. \qquad (4)$$

Consider the midpoint in this nebula, where the H^0 fraction is roughly 6×10^{-4}. The hydrogen density is 1×10^4 cm^{-3} so the H^0 density is 6 cm^{-3}. The hydrogen photoionization cross section near threshold is $\sigma(H^0) = 6 \times 10^{-18}$ cm^{-2} so the mean free path of a hydrogen ionizing photon is $\lambda_{912} \approx 2.8 \times 10^{16}$ cm. The heating cannot change over length scales smaller than this, the mean free path of an ionizing photon. This is summarized in Table 2, which lists cross sections and timescales for thermal (1×10^4 K ~ 1 eV) particles.

Next consider the electron mean free path. The electron density is 1.1×10^4 cm^{-3} if He is singly ionized. The electron - electron collision cross section is 0.8×10^{-12} / T(eV)^2 cm^2 (equation 198 of Kulsrud 2005). Take 10 eV for the photoelectron

TABLE 2

LENGTH AND TIME SCALES IN THE ORION H II REGION.

Particle	Density $\left[\text{cm}^{-3}\right]$	Cross section $\left[\text{cm}^2\right]$	$n \times \sigma$	time (s)
e-e	1.1×10^4	1×10^{-12}	1×10^{-10}	2
Protons	1×10^4	3×10^{-23}	3×10^{-19}	6×10^{10}
He$^+$	1×10^3	4×10^{-23}	4×10^{-20}	5×10^{11}
e+O^{2+}, $h\nu$	3	1×10^{-18}	3×10^{-18}	6×10^9

initial energy. This is a very high energy for an O star photoelectron (see Table 1) but will favor the importance of non-thermal "kappa" electrons. The electron mean free path is then $\lambda_{e-e} \approx 1.1 \times 10^{10} \left(T(eV)/10 \ eV\right)^2$ cm, 6.4 dex smaller than the heating scale length. The heating is constant over physical scales far larger than the distance between thermalizing electron collisions. This distinguishes H II regions from neutral regions of shocks where the mean free path can be long.

Next compare the heating timescale and the electron thermalization timescale. Assuming photoionization equilibrium and that the ionization / recombination rates are equal, the heating rate is $(h\nu - h\nu_o)n_e n_p \alpha_B$ (AGN3). For the same parameters, and a temperature of $T_e = 1 \times 10^4$ K, the heating rate is then 10 eV $\times 1.1 \times 10^4$ cm^{-3} $\times 1.0 \times 10^4$ cm^{-3} $\times 2.6 \times 10^{-13}$ cm^3 s^{-1} = 2.9×10^{-4} eV cm^{-3} s^{-1} for these parameters. The heat content of the gas is $3/2$ nkT = $1.5 \times 2.2 \times 10^4 \times 8.6 \times 10^{-5} \times 1 \times 10^4$ = 2.8×10^4 eV cm^{-3}. The heating timescale is the ratio, $2.84 \times 10^4 / 2.9 \times 10^{-4}$ = 9.7×10^7 s, about three years.

The time for electrons to approach a Maxwellian is given by Spitzer (1962) equation 5-26 for the "self-collision time":

$$t_c = \frac{m^{1/2}(3kT)^{3/2}}{8 \times 0.714\pi n e^4 Z^4 \log \Lambda} = \frac{11.4A^{1/2}T^{3/2}}{nZ^4 \log \Lambda}\text{s}. \quad (5)$$

Assuming $n_e = 1.1 \times 10^4$ cm^{-3} and Spitzer's numbers the thermalization timescale is ~ 2 s. The electrons approach a Maxwellian on a timescale 8×10^7 times faster than the heating time. The heating is constant over times far longer than the time needed to set up a Maxwellian. This is unlike the solar flare case, where heating rates change very quickly.

These two estimates show that the distance an electron travels before becoming thermal is 6.5 dex shorter than the scale length heating over which the heating changes, and that the electron Maxwellian timescale is nearly 8 dex faster than the heating timescale. These establish that the electron velocity distribution has time to closely maintain a Maxwellian at the local kinetic temperature.

5. WHAT IF THERE ARE NON-THERMAL ELECTRONS IN THE IONIZED GAS?

Suppose that a non-photoionization process allows high-energy electrons to exist in the ionized gas. The electron thermalization cross section decreases as E^{-3}, so higher energy electrons are more difficult to thermalize. Could these high-energy non-thermal electrons produce forbidden line emission before becoming thermalized?

The non-thermal electron would have to have an inelastic collision with an O^{2+} ion and collisionally excite the 500.7 nm [O III] line before it is thermalized by collisions with other electrons for this process to make any sense. The cross section for an e-e collision is given by Kulsrud equation 198, 0.8×10^{-14} / T(eV)^2 cm^2 while cross section for an e - O^{2+} collision that produces the 500.7 nm line is 1×10^{-18} cm^2 at thermal energies, assuming the collision strengths in Lennon & Burke (1994). The cross section for exciting a forbidden line falls off as E^{-3} at high energies (Burgess & Tully 1992) while the e-e cross section falls off as E^{-2}. These are shown in Figure 4. Assuming a solar O/H, that all O is O^{2+}, and $n_e = 1.1n_H$, we obtain $n_e/n_{O^{2+}} = 2.2 \times 10^3$. Evaluating the cross sections at 10 keV we find that an energetic electron will have $\sim 10^8$ thermalizing collisions with other electrons before it can strike an O^{2+}.

The result is that an energetic electron will undergo a very large number of thermalizing collisions long before it can strike an O^{2+} ion. The only scenario where the non-thermal electron can strike an O^{2+} and produce light before undergoing a thermalizing e-e collision would be one where the O/H ratio is 7 dex or more above solar.

Cosmic rays will add kinetic energy to an ionized gas. They create a significant population of non-thermal secondaries in a neutral medium (Spitzer & Tomasko 1968), but that is not the state of an H II region, which is highly ionized. Given the energy dependencies of the ratio of cross sections given above, very high-energy particles will be even less likely to directly excite [O III] lines. The energy available in cosmic rays is small compared to the energy in
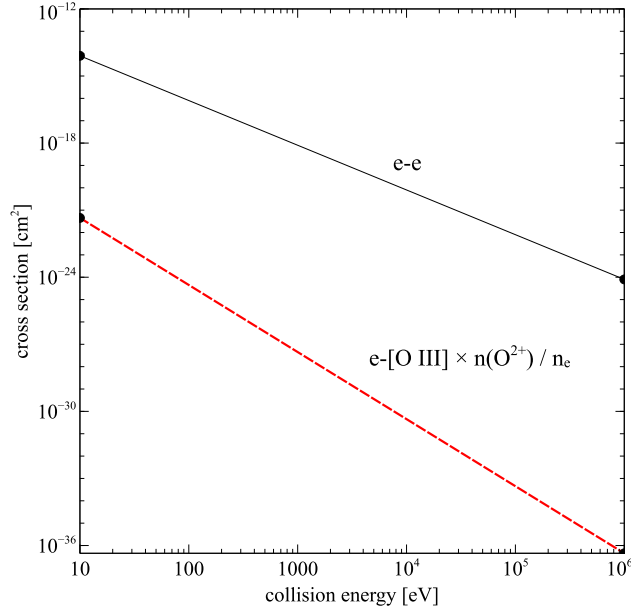
Fig. 4. This compares the e-e collision cross section with the cross section for exciting the O III green line.

starlight in a typical nebula.

6. CONCLUSIONS

As discussed in the Introduction, many explanations have been offered for the t^2/ADF phenomenon, and different processes may operate in different objects. This paper investigates the possibility that a significant population of non-thermal electrons might be present in ionized regions of nebulae, and that these disturb the line ratio diagnostics. Photoionization does produce supra-thermal electrons that are much more energetic than thermal electrons. Cosmic rays or other high-energy particles may also be present.

We do a quantitative evaluation of the time it takes to thermalize such energetic electrons, and the distances they move in this time. We have used well established methods to show that the thermalization distances and timescales are much smaller than the distance or time in which the heating or temperature can vary. These suggest that supra thermal electrons will have disappeared into the Maxwellian velocity distribution long before they affect the collisionally excited forbidden and recombination lines that we use for deriving relative abundances We know of no numerical calculations that follow the thermalization of electrons in an ionized gas, probably because these comparisons suggest that a Maxwellian velocity distribution will result. These considerations strongly suggest that non-thermal electrons should

not be important and cannot account for t^2/ADF phenomenon. Therefore, to explain the observed ADF values in photoionized nebulae, other t^2 producing phenomena must be considered.

Emission line ratios can probe the existence of non-thermal electrons (Bradshaw & Raymond 2013). Storey & Sochi (2013) considered C II lines formed by dielectronic recombination and did not find strong evidence for a kappa distribution. Mendoza & Bautista (2014) consider line ratios, including uncertainties in the atomic data, and also find no evidence for kappa distributions in nebulae. Similarly, Zhang et al. (2016) find no evidence of kappa in a sample of H II regions and planetary nebulae. A study of H I emission in Hf 2-2 by Storey & Sochi (2014) finds no evidence of kappa. Observations support the conclusion that kappa distributions have negligible effect in nebulae.

This work has focused on the Orion H II region, the brightest and best-studied nebula. A future paper, Henney et al. (in preparation) will extend this analysis to more general cases, including planetary nebulae and extragalactic H II regions. Quantitative calculations of the deviation from a Maxwellian velocity distribution due to the injection of high-energy electrons will be presented.

REFERENCES

Baldwin, J. A., Ferland, G. J., Martin, P. G., Corbin, M. R., Cota, S. A., Peterson, B. M., & Slettebak, A. 1991, ApJ, 374, 580

Bergeron, J., & Collin-Souffrin, S. 1973, A&A, 25, 1

Bhatnagar, P. L., Gross, E. P., & Krook, M. 1954, Physical Review, 94, 511

Bohm, D., & Aller, L. H. 1947, ApJ, 105, 131

Bradshaw, S. J., & Raymond, J. 2013, Space Sci. Rev., 178, 271

Burgess, A., & Tully, J. A. 1992, A&A, 254, 436

Dalgarno, A., Yan, M., & Liu, W. 1999, ApJS, 125, 237

Dopita, M. A., Sutherland, R. S., Nicholls, D. C., Kewley, L. J., & Vogt, F. P. A. 2013, ApJS, 208, 10

Esteban, C., Peimbert, M., García-Rojas, J., Ruiz, M. T., Peimbert, A., & Rodríguez, M. 2004, MNRAS, 355, 229

Ferland, G. J. 2001, PASP, 113, 41

—. 2003, ARA&A, 41, 517

Ferland, G. J., et al. 2013, Revista Mexicana de Astronomia y Astrofisica, 49, 137

Kulsrud, R. M. 2005, Plasma physics for astrophysics

Lennon, D. J., & Burke, V. M. 1994, A&AS, 103, 273

Liu, X.-W., Storey, P. J., Barlow, M. J., Danziger, I. J., Cohen, M., & Bryce, M. 2000, MNRAS, 312, 585

Maloney, P. R., Hollenbach, D. J., & Tielens, A. G. G. M. 1996, ApJ, 466, 561

Mendoza, C., & Bautista, M. A. 2014, ApJ, 785, 91

Nicholls, D. C., Dopita, M. A., & Sutherland, R. S. 2012, ApJ, 752, 148

Nicholls, D. C., Dopita, M. A., Sutherland, R. S., Kewley, L. J., & Palay, E. 2013, ApJS, 207, 21

Osterbrock, D. E. 2002, in Revista Mexicana de Astronomia y Astrofisica Conference Series, Vol. 12, Revista Mexicana de Astronomia y Astrofisica Conference Series, ed. W. J. Henney, J. Franco, & M. Martos, 1–7

Osterbrock, D. E., & Ferland, G. J. 2006, Astrophysics of gaseous nebulae and active galactic nuclei, 2nd. ed. (Sausalito, CA: University Science Books)

Peimbert, A. 2003, ApJ, 584, 735

Peimbert, A., & Peimbert, M. 2013, ApJ, 778, 89

Peimbert, M. 1967, ApJ, 150, 825

Peimbert, M., Storey, P. J., & Torres-Peimbert, S. 1993, ApJ, 414, 626

Raymond, J. C., Isenberg, P. A., & Laming, J. M. 2008, ApJ, 682, 408

Shull, J. M. 1979, ApJ, 234, 761

Shull, J. M., & van Steenberg, M. E. 1985, ApJ, 298, 268

Spitzer, L. 1962, Physics of Fully Ionized Gases (2nd edition) (New York: Interscience)

—. 1978, Physical processes in the interstellar medium (New York Wiley-Interscience), 333 p.

Spitzer, L., & Härm, R. 1953, Physical Review, 89, 977

Spitzer, L. J., & Tomasko, M. G. 1968, ApJ, 152, 971

Storey, P. J., & Sochi, T. 2013, MNRAS, 430, 599

—. 2014, MNRAS, 440, 2581

Vasyliunas, V. M. 1968, J. Geophys. Res., 73, 2839

Xu, Y., & McCray, R. 1991, ApJ, 375, 190

Zhang, Y., Zhang, B., & Liu, X.-W. 2016, ApJ, 817, 68

G. J. Ferland: Department of Physics and Astronomy, University of Kentucky, Lexington, KY 40506, USA

W. J. Henney: Centro de Radioastronomía y Astrofísica, Universidad Nacional Autónoma de México, Apartado Postal 3-72, 58090 Morelia, Michoacán, México

C. R. O'Dell: Department of Physics and Astronomy, Vanderbilt University, Box 1807-B, Nashville, TN 37235

M. Peimbert Instituto de Astronomia, Universidad Nacional Autónoma de México, Apdo, Postal 70-264, 04510 México D. F., México